Supporting Information

Precisely tailoring Lewis Pairs in polyoxotitanium clusters for efficient photocatalytic production of hydrogen peroxide

Mengke Gao[ab], Shiming Zhang[a], Yayu Yan[a], Zehao Qian[a], Liyang Qin[a], Xiaoyu Liu[ab], Qing-Rong Ding[a], Qiaohong Li[a], Xin Wu*[a] and Jian Zhang*[a]

[a] State Key Laboratory of Structural Chemistry, Fujian Institute of Research on the Structure of Matter.Email: zhj@fjirsm.ac.cn

[b] Chinese Academy of Sciences, Fuzhou, Fujian 350002, P. R. China; College of Chemistry and Materials Science, Fujian Normal University, Fuzhou, Fujian 350007

Materials and Reagents

All reagents and solvents were purchased commercially and used without further purification. $Ti(OiPr)_4$, adenine, and cobalt acetate hexahydrate were obtained from Adamas-beta; phenylphosphonic acid and manganese acetylacetonate were purchased from Energy Chemical; and isopropanol (99.7%) was acquired from Sinopharm Chemical Reagent.

Characterization

Crystallographic data of Ti_3Co cluster and Ti_3Mn cluster were collected on a Supernova single crystal diffractometer equipped with graphite-monochromatic Ga-Kα radiation (λ = 1.54178 Å) at 293 K.Powder X-ray diffraction (PXRD) data was collected at 40 kV, 30 mA using microcrystalline samples on a Rigaku Ultima IV diffractometer using Ga-Kα radiation(λ = 1.34139 Å). The measurement parameters include a scan speed of 3 °/min, a step size of 0.02°, and a scan range of 2θ from 3° to 50°. Fourier transform infrared spectroscopy (FT-IR) data were collected on a PerkinElmer Spectrum 100 FT-IR Spectrometer. UV-Vis absorption spectra were measured on a Perkin-Elmer Lambda 35 UV-Vis spectrophotometer. Thermogravimetric analyses (TGA) were performed on a Mettler Toledo TGA/SDTA 851e analyzer in N_2 atmosphere with a heating rate of 10°C /min from 20 °C to 800 °C.

Synthesis of Ti_3Co cluster:

Synthesis of Ti_3Co cluster： A mixture of phenylphosphonic acid (0.1050 g, 0.66 mmol), adenine (0.0300 g, 0.25 mmol), pyrazine (0.0150 g, 0.19mmol)and cobaltous nitrate hexahydrate (0.0300 g, 0.085 mmol) and $Ti(OiPr)_4$ (0.92 mL) are dissolved in isopropanol (5.5 mL) in a 20 mL scintillation vial, heated at 100 °C for 4 days, and then cooled to room temperature. Violet lumpy crystals of Ti_3Co are obtained and dried in air (59% yield, based on Ti).

Synthesis of Ti_3Mn cluster:

Synthesis of Ti_3Mn cluster： A mixture of phenylphosphonic acid (0.1050 g, 0.66 mmol), adenine (0.0300 g, 0.25 mmol), pyrazine (0.0150 g, 0.19 mmol)and manganese acetylacetonate (0.0300 g, 0.085 mmol)and $Ti(OiPr)_4$ (0.92 mL) are dissolved in isopropanol (5.5 mL) in a 20 mL scintillation vial, heated at 100 °C or 4 days, and then cooled to room temperature. Brown lumpy crystals of Ti_3Mn are obtained and dried in air (62% yield, based on Ti).

Photocatalytic H_2O_2 production：

Photocatalytic H_2O_2 production experiments were conducted in a sealed quartz reaction tube at ambient temperature. A 300 W xenon lamp (PLS-SXE 300D, full-spectrum output with UV-visible components) was used as the light source without optical filters. In a typical experiment, 10 mg of photocatalyst was dispersed in 10 mL of a mixed solution of IPA and deionized water (volume ratio H_2O:IPA = 1:9). IPA served as a hole scavenger to enhance charge separation efficiency. Prior to light irradiation, the system was purged with high-purity O_2 gas for 30 min to saturate the solution with dissolved oxygen, which acts as the electron acceptor for the oxygen reduction reaction (ORR). To detect H_2O_2 formation, 2 mL of the suspension was withdrawn and filtered through a 0.22 μm membrane to obtain a transparent solution for subsequent H_2O_2 detection.[1, 2]

Photoeletrochemical measurements:

Photocurrent and Mott-Schottky measurements were made in 0.5 M sodium sulfate solution (pH=6.8) through the traditional three-electrode system in the CHI 760E electrochemical workstation. During the measurements, an Ag/AgCl electrode was used as the reference electrode, and a Pt foil electrode acted as the counter electrode.The working electrodes were designed using resulting samples covered on the surface of fluoride tin oxide (FTO) conductor glass. For electrochemical impedance spectroscopy (EIS) measurements, a quartz cell filled with 0.5 M Na_2SO_4 (pH=6.8) electrolyte was used as the measurement system, with a sine wave with an amplitude of 5 mV and a frequency range of 100 kHz to 0.05Hz.

Computational methods:

Orbitals and density of states (DOS) calculations based on density functional theory (DFT) through Vienna Ab initio Simulation Package (VASP)[3]. Projector augmented wave (PAW)[4] potentials were employed for modeling electron-ion interactions. The generalized gradient approximation with the Per-dew-Burke-Ernzerhof (GGA/PBE)[5] was used for calculations. The convergence criteria and the cutoff energy of plane wave basis were 1×10^{-4} eV and 450 eV, respectively. The threshold for force was set to -0.02 eV·$Å^{-1}$. And the Van der Waals (vdW) correction was adopted by Grimme (DFT+D3). The VESTA[4] software and vaspkit[7] applet was used for data processing. Electrostatic potential calculation was implemented in Gaussian 16. The structural model is optimized by using B3LYP Functionals, C, H, P, O and N using 6-31G(d,p) basis sets, Co and Ti using Lanl2DZ basis sets, and D3 dispersion correction of Grimme, with D3 dispersion correction of Grimme. [8-13]

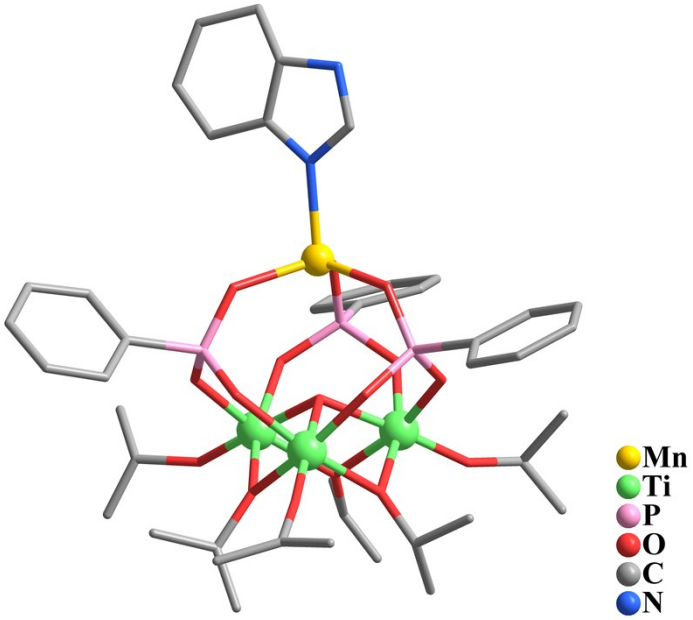

Figure S1 Crystal structure of Ti_3Mn cluster.

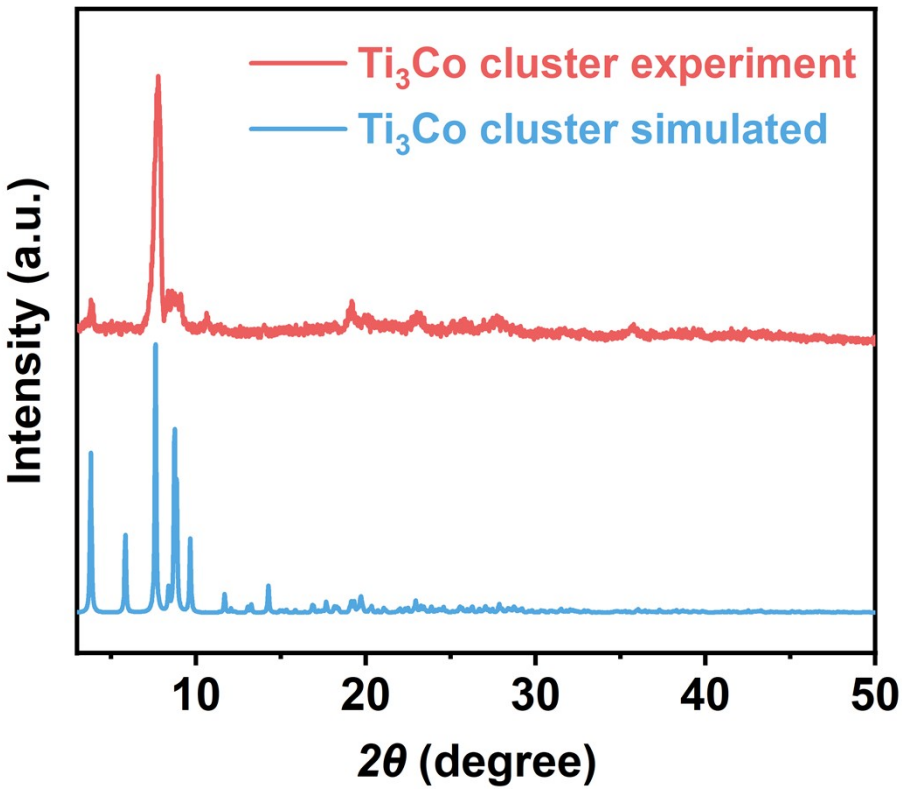

Figure S2 The PXRD of the simulated and experimental patterns of Ti_3Co cluster.

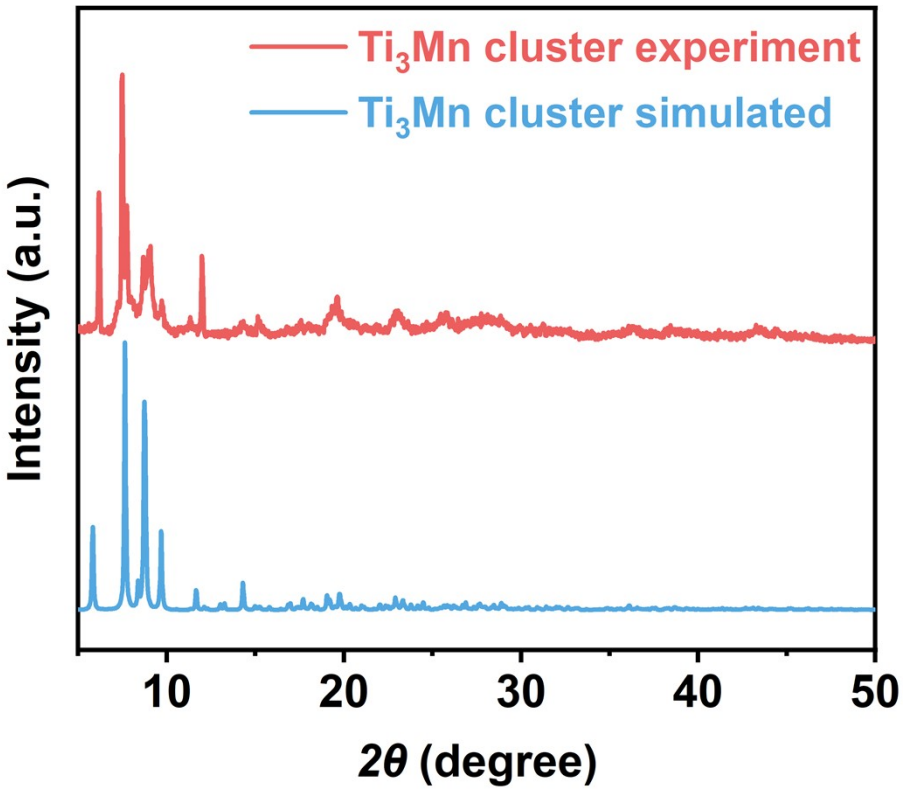

Figure S3 The PXRD of the simulated and experimental patterns of Ti_3Mn cluster.

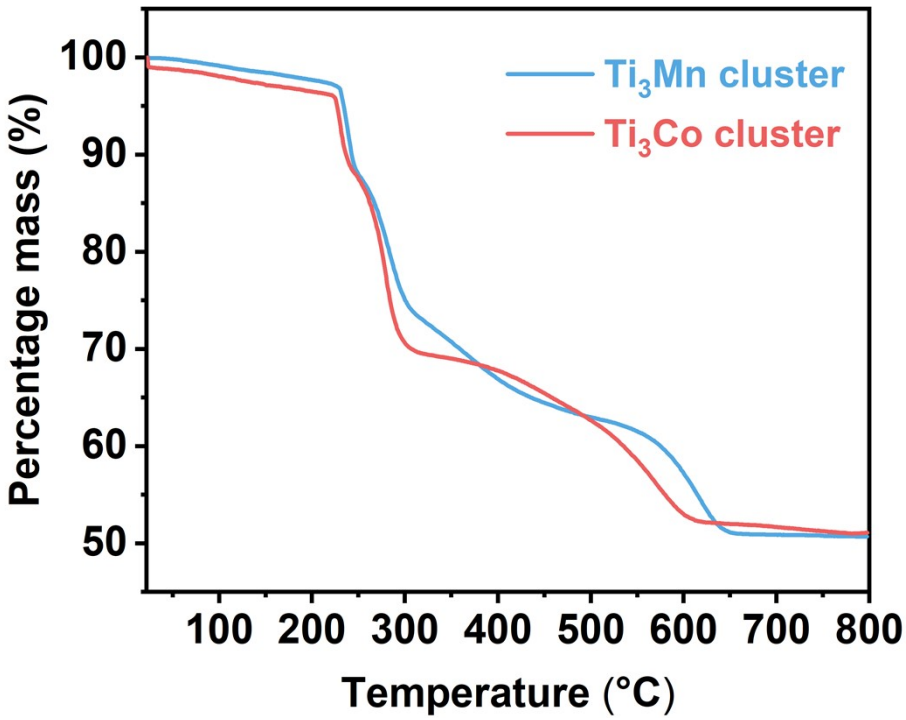

Figure S4 The TGA curves of Ti_3Mn cluster and Ti_3Co cluster.

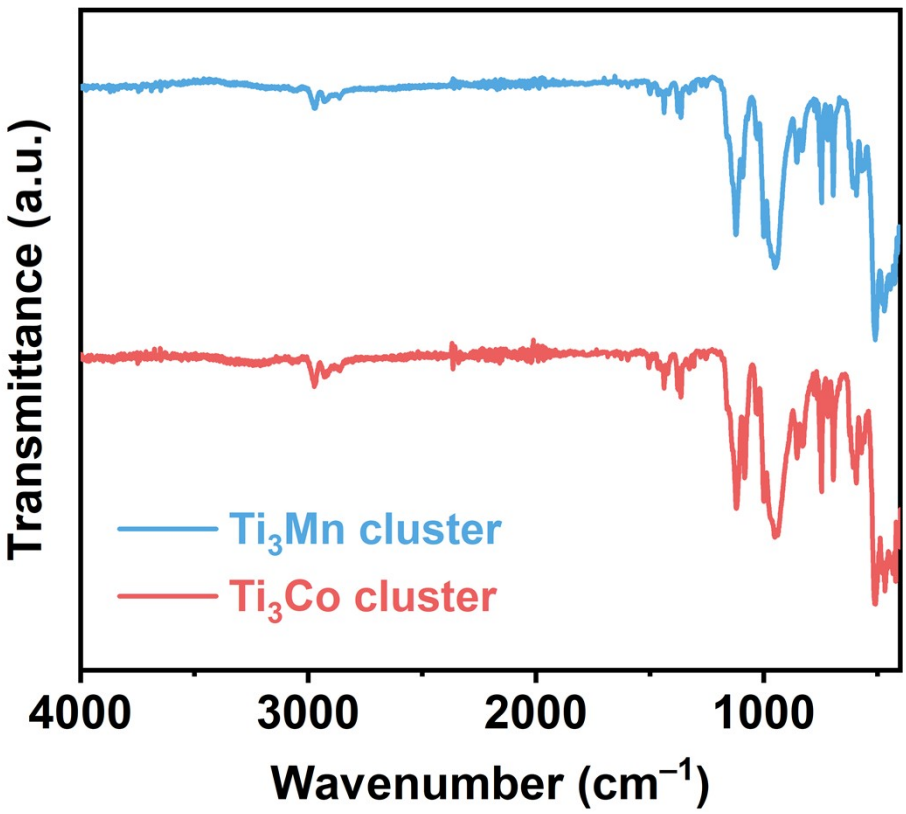

Figure S5 The FT-IR spectra of Ti_3Mn cluster and Ti_3Co cluster.

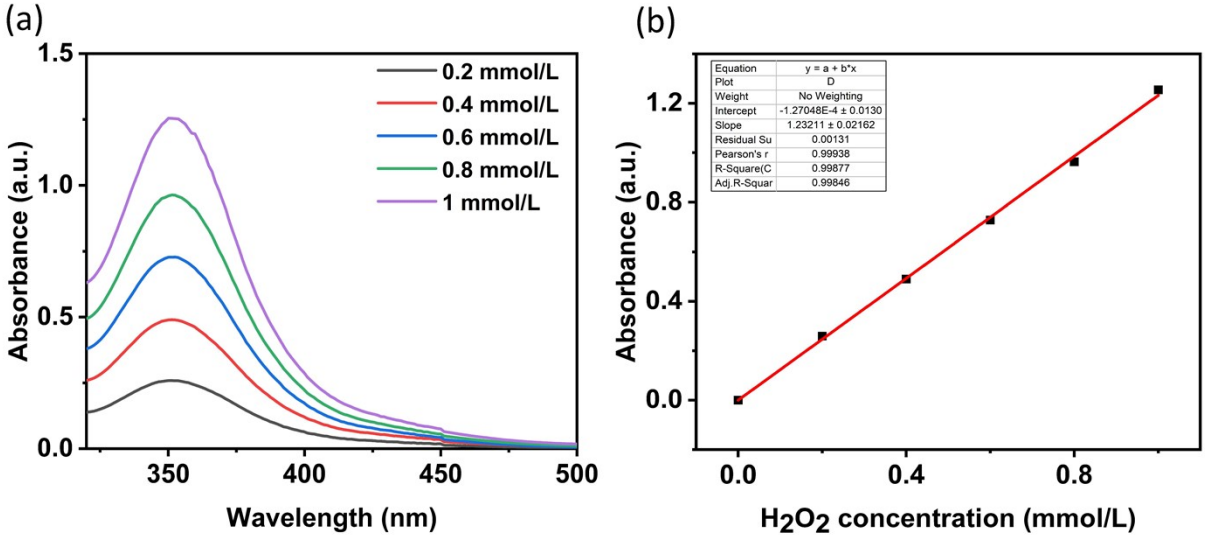

Figure S6 The standard curve of H_2O_2 concentration-absorbance by Iodometry.
(a) UV-Vis absorption spectra of H_2O_2 solutions with different concentrations.
(b) The H_2O_2 concentration - absorbance standard curve.

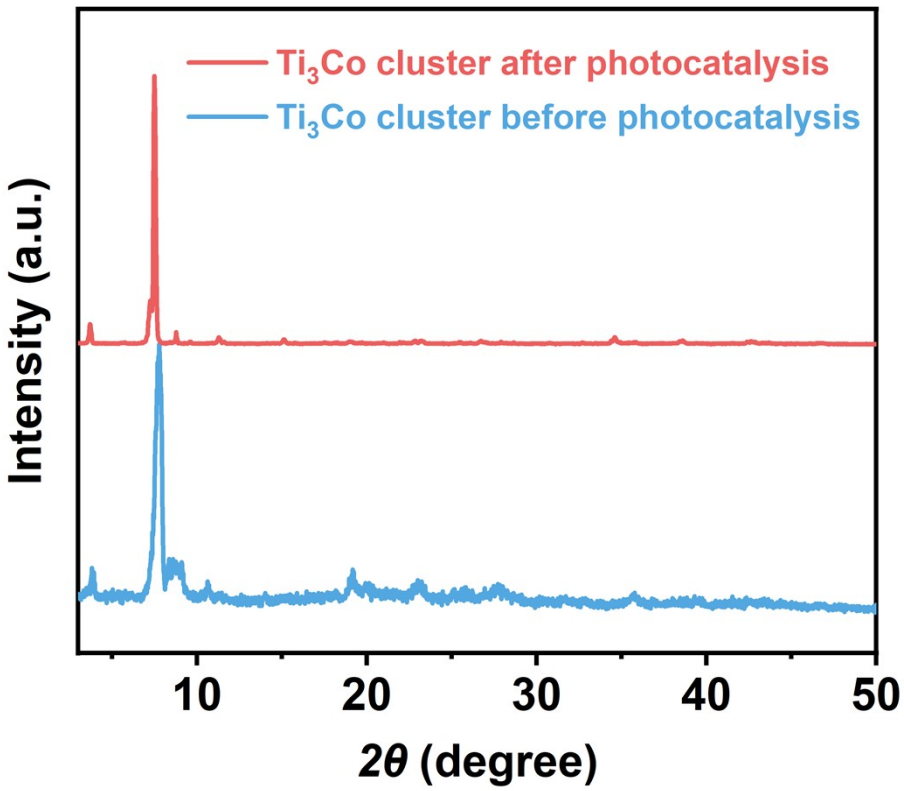

Figure S7 The PXRD patterns of Ti_3Co cluster after photocatalytic test.

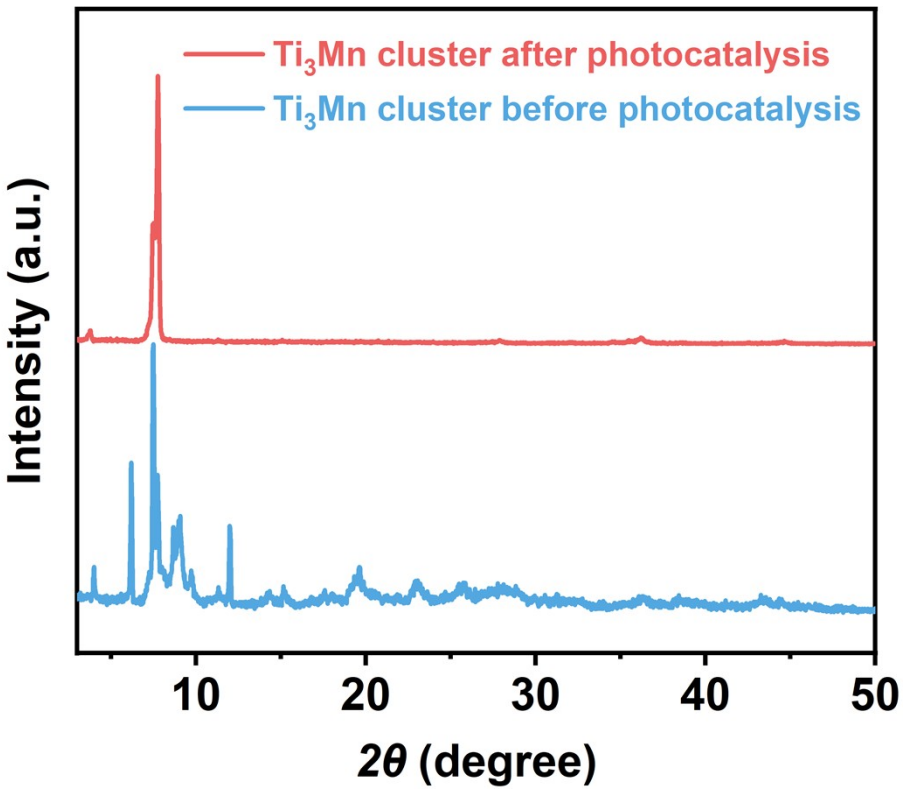

Figure S8 The PXRD patterns of Ti_3Mn cluster after photocatalytic test.

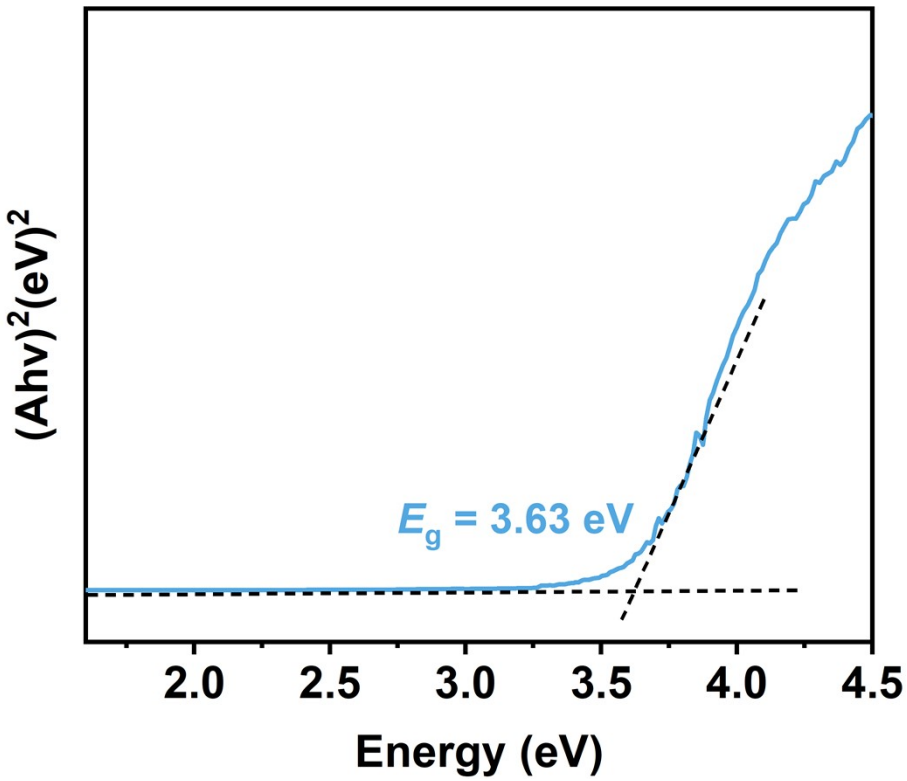

Figure S9 Tauc plot for band gap calculation of Ti_3Mn cluster.

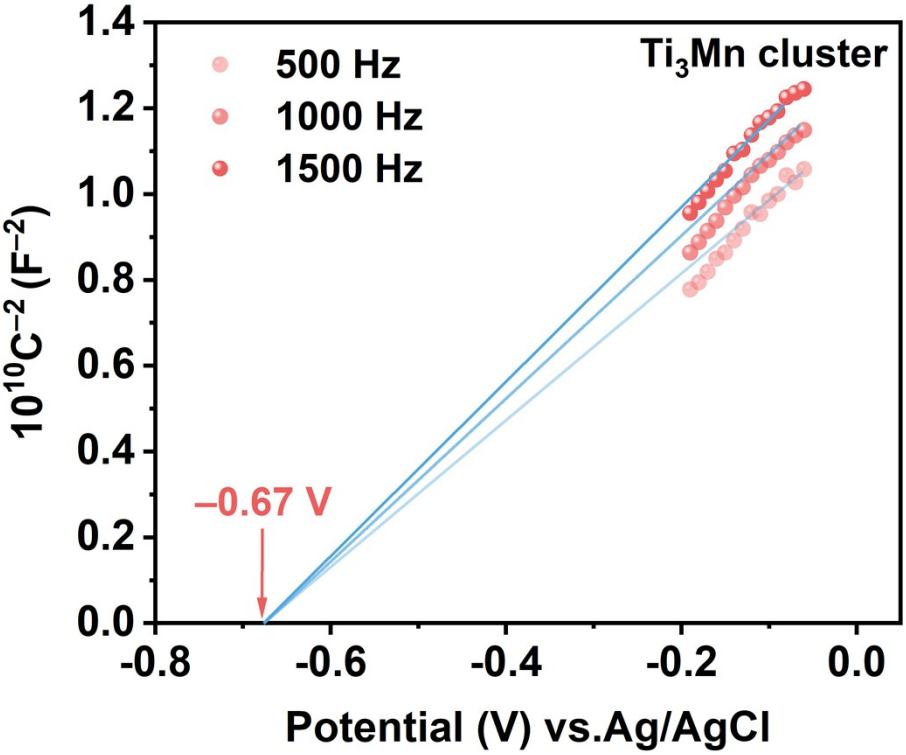

Figure S10 Mott-Schottky plots for Ti_3Mn cluster.

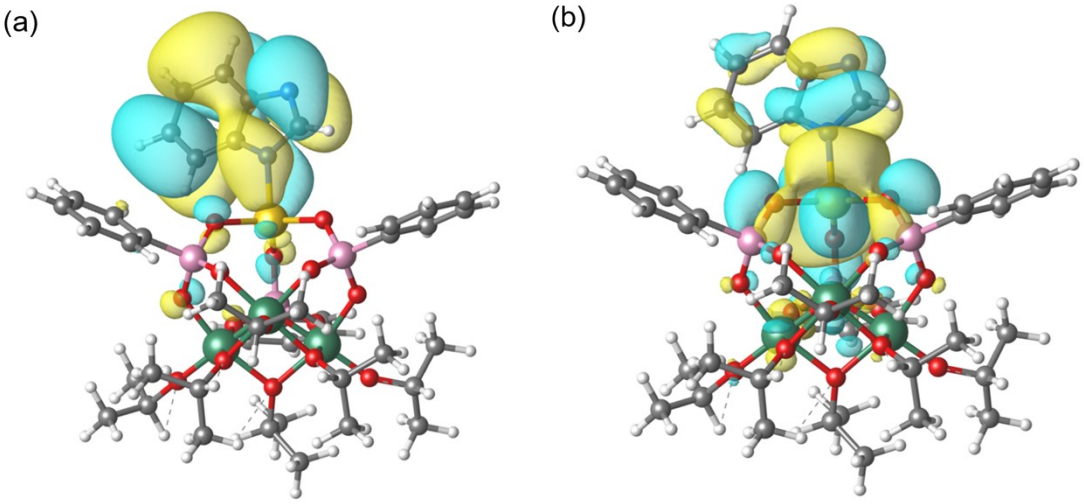

Figure S11 (a) The HOMO of Ti_3Mn cluster. (b)The LUMO of Ti_3Mn cluster.

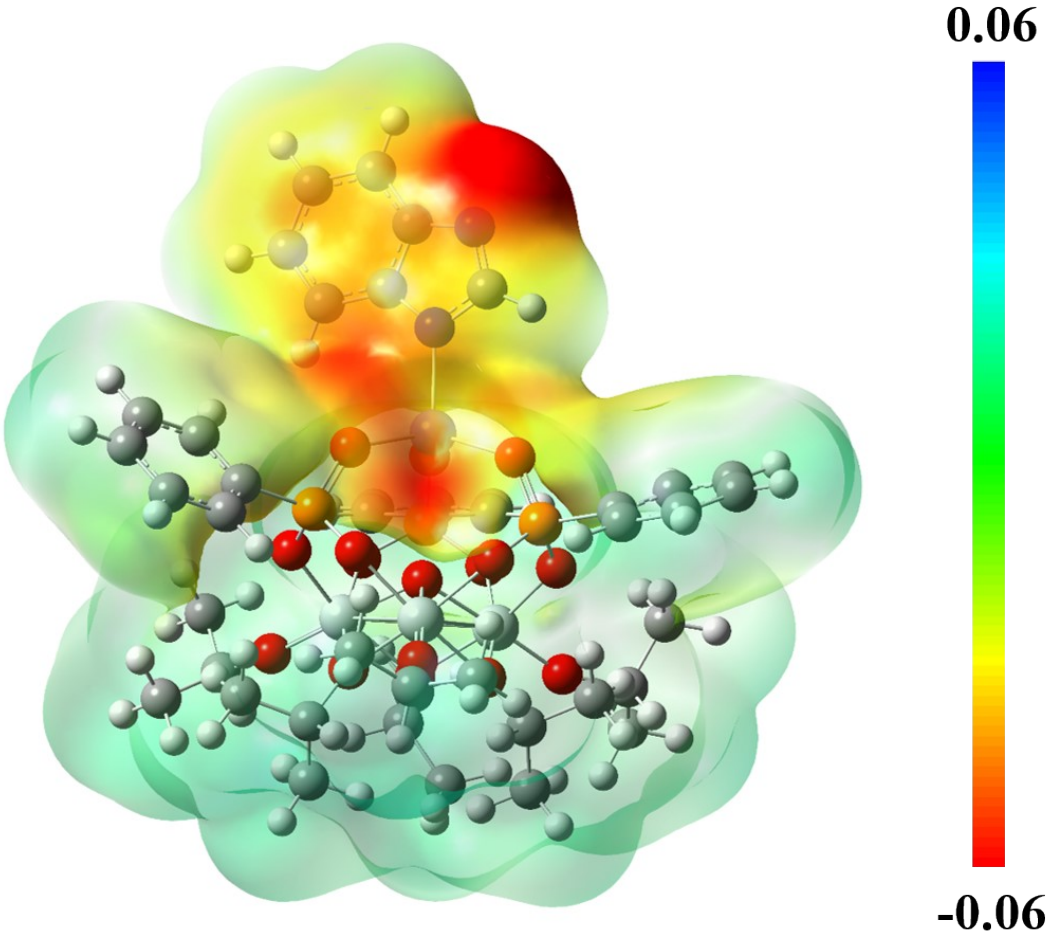

Figure S12 Electrostatic potential of Ti_3Mn cluster.

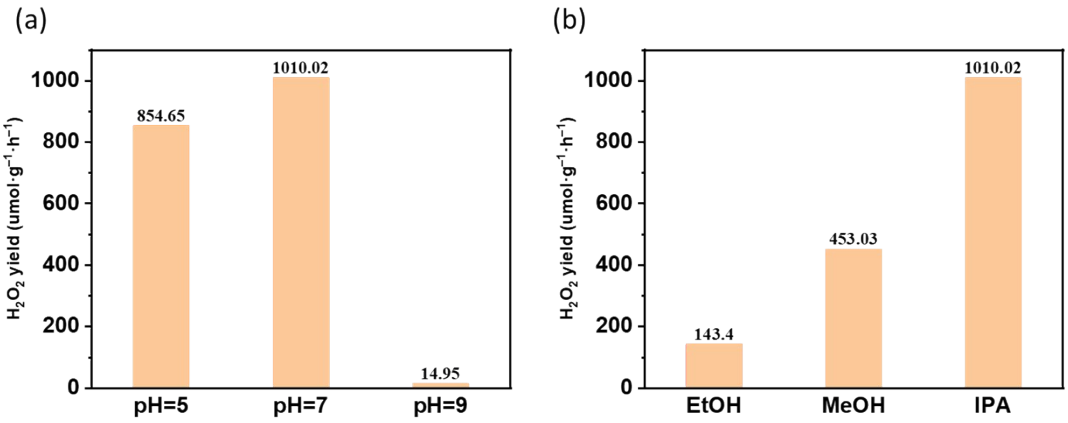

Figure S13 (a) H_2O_2 production under different pH. (b) H_2O_2 production under different proton donor solvents.

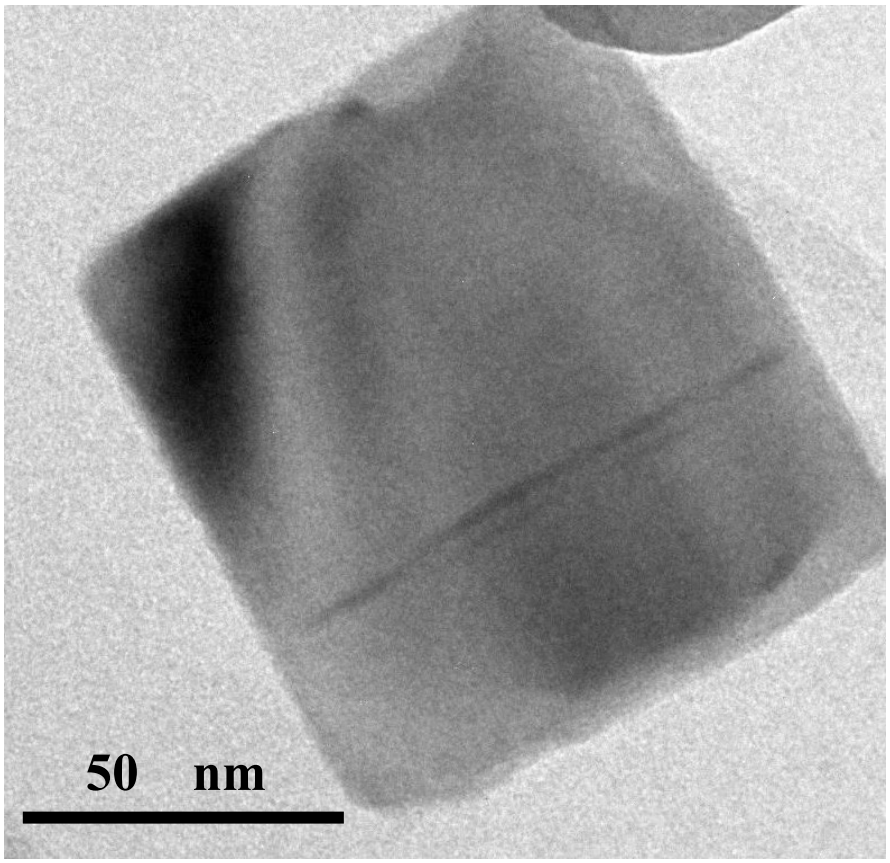

Figure S14 TEM of Ti_3Co cluster.

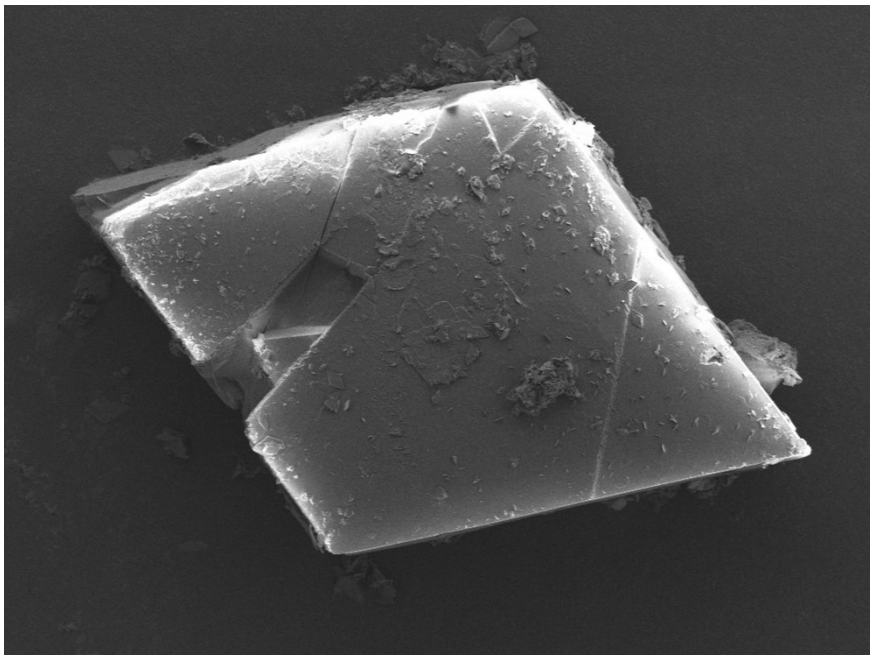

Figure S15 SEM of Ti_3Co cluster.

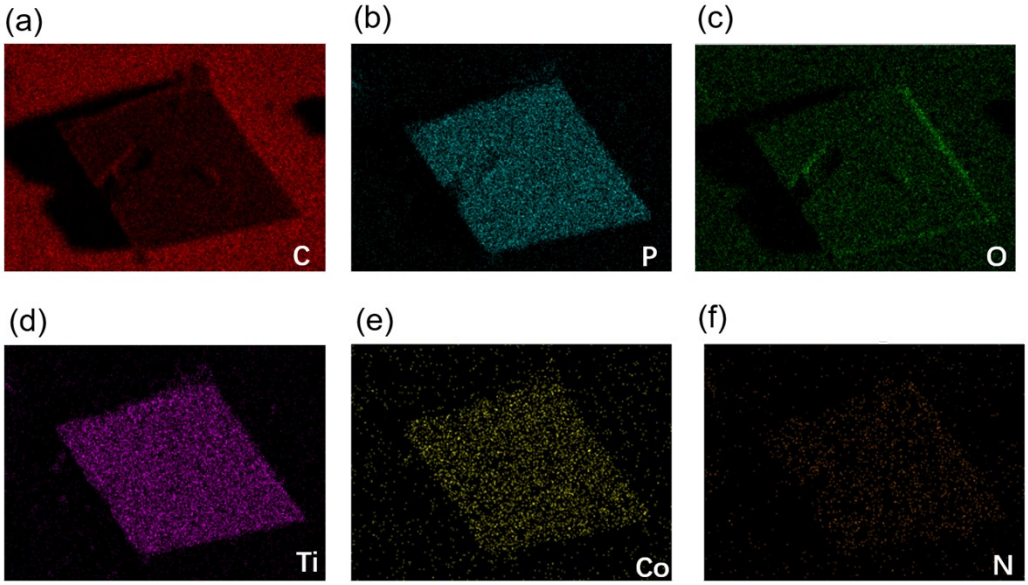

Figure S16 EDS of Ti_3Co cluster (a)showing the uniform distribution of elements C (b) P, (c) O, (d) Ti, (e) Co, and (f) N.

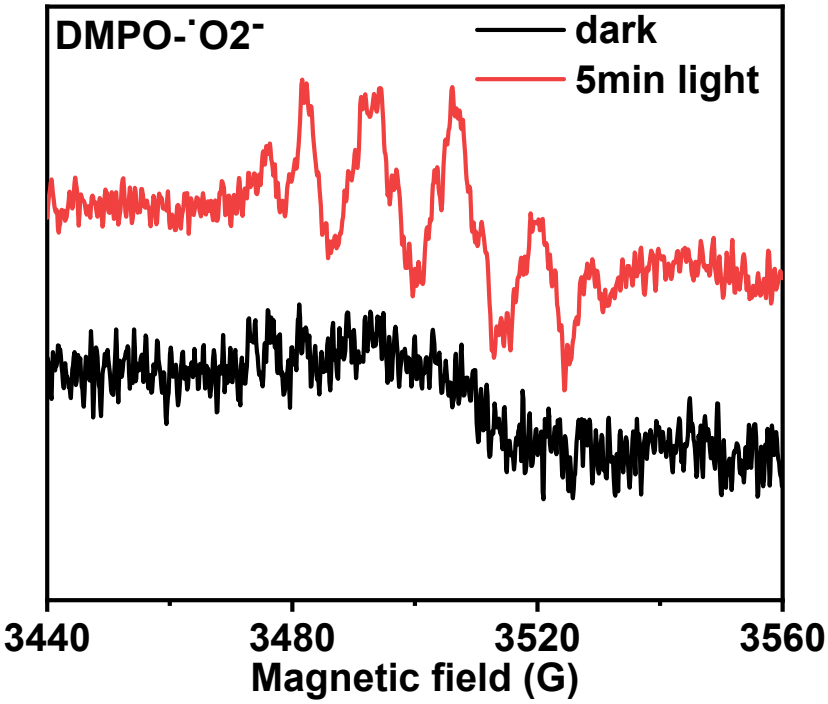

Figure S17 EPR trapping experiments of Ti_3Co cluster.

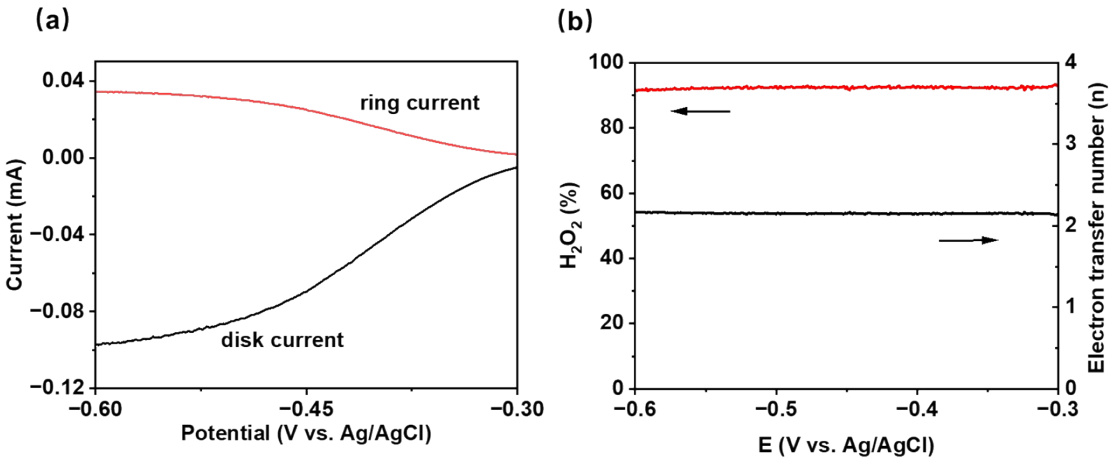

Figure S18 RRDE measurements of Ti_3Co cluster.

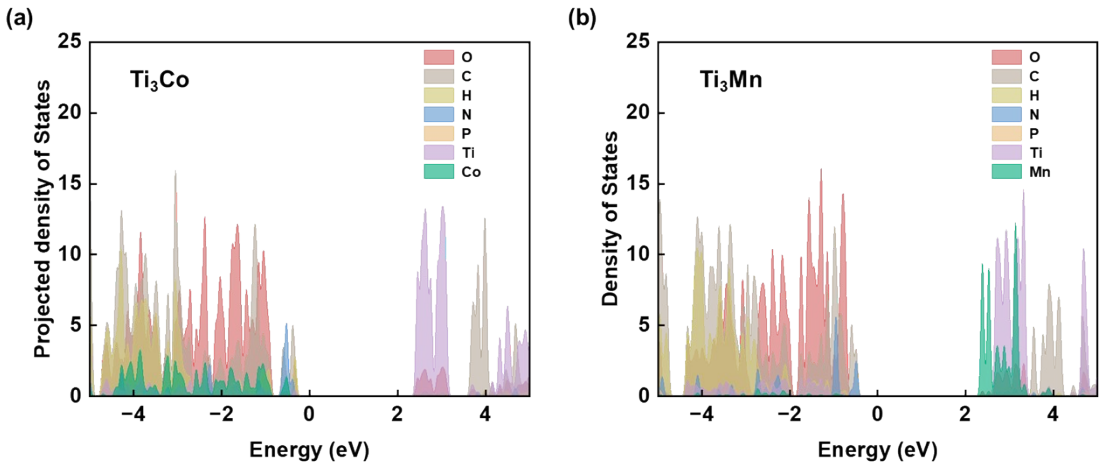

Figure S19 Projected density of states of Ti_3Co cluster (a) and Ti_3Mn cluster (b).

Table S1. Crystallographic data and structure refinement results for **1** and **2**.

Empirical formula	$C_{43}H_{59.8}MnN_2O_{16}P_3Ti_3$ (**1**)	$C_{43}H_{58}CoN_2O_{16}P_3Ti_3$ (**2**)
Identification code	Ti_3Mn cluster	Ti_3Co cluster
CCDC number	2407618	2407617
Formula weight	1152.27	1154.45
Temperature (K)	293(2)	293(2)
Wavelength	1.34139	1.3405
Crystal system	Monoclinic	Monoclinic
Space group	$P2_1/c$	$P2_1/c$
a (Å)	23.4156(6)	23.5030(3)
b (Å)	20.0918(4)	19.9604(2)
c (Å)	12.5358(3)	12.5665(10)
α (°)	90	90
β (°)	99.326(2)	99.004(2)
γ (°)	90	90
Volume (Å^3)	5819.7(2)	5822.67(16)
Z	4	4
Density (calculated) (g cm^{-3})	1.315	1.317
Absorption coefficient (mm^{-1})	6.396	6.860
F (000)	2383	2384
Crystal size (mm^3)	0.02 × 0.02 × 0.02	0.1 × 0.1 × 0.1
Theta range for data collection (°)	3.824–160.114	3.806–160.28
Reflections collected	44446	44488
Independent reflections	12049 [R(int) = 0.0443]	12055 [R(int) = 0.0412]
Completeness to theta=160.114°	0.999	0.996
Refinement method	Full-matrix least-squares on F^2	Full-matrix least-squares on F^2
Data/restraints/parameters	12049/432/757	12055/288/635
Goodness-of-fit on F^2	1.045	1.075
$R_1{}^a$ [$I \geq 2\sigma(I)$]	0.0717	0.0670
$wR_2{}^b$ [$I \geq 2\sigma(I)$]	0.2031	0.2089
$R_1{}^a$ [all data]	0.0860	0.0767
$wR_2{}^b$ [all data]	0.2150	0.2274
Largest diff. peak/hole/e Å^{-3}	1.32/–0.56	1.40/-0.81

$^{(a)}R_1 = \Sigma||F_o|-|F_c||/\Sigma|F_o|$, $^{(b)}wR_2 = (\Sigma(w(F_o^2-F_c^2)^2)/\Sigma(w(F_o^2)^2))^{1/2}$.

Table S2 Valence bond analysis of Ti_3Co cluster.

Co01	1.794	Ti01	4.137
		Ti03-O008	0.665
Co01-O00G	0.479	Ti03O00A	0.621
Co01-O00H	0.491	Ti03-O00C	0.642
Co01-O00I	0.476	Ti03-O00F	0.594
Co01-N00O	0.348	Ti03-O00K	0.570
		Ti03-O00M	1.157
Ti02	4.2333	Ti03	4.169
Ti02-O008	0.627	Ti04-O008	0.637
Ti02-O009	0.635	Ti04-O00D	0.573
Ti02-O00B	0.642	Ti04-O00E	0.661
Ti02-O00D	0.582	Ti04-O00J	0.691
Ti02-O00F	0.561	Ti04-O00K	0.533
Ti02-O00L	1.123	Ti04-O00N	1.117

Table S3 Valence bond analysis of Ti_3Mn cluster.

Mn01	2.007	Ti01	4.237
		Ti01-O16	0.644
Mn01-O06	0.514	Ti01-O02	0.633
Mn01-O03	0.526	Ti01-O15	0.584
Mn01-O09	0.513	Ti01-O04	0.644
Mn01-N01	0.454	Ti01-O11	0.572
		Ti01-O10	1.160
Ti02	4.17	Ti03	4.217
Ti02-O16	0.627	Ti03-O16	0.637
Ti02-O01	0.635	Ti03-O15	0.573
Ti02-O07	0.642	Ti03-O05	0.661
Ti02-O11	0.582	Ti03-O08	0.691
Ti02-O13	0.561	Ti03-O13	0.533
Ti02-O12	1.123	Ti03-O14	1.117

Table S4. Cobalt content in the reaction filtrate.

Sample	Average concentration	Amount of Co
Ti_3Co cluster	0.505 mg/L	0.00505mg

Table S5. Elemental analysis results before and after Ti_3Co cluster photocatalysis.

Sample	N(%)	C(%)	H(%)
Ti_3Co-before photocatalysis	2.327	42.225	5.772
Ti_3Co-after photocatalysis	2.274	42.748	6.144

Table S6. Apparent Quantum Yield and SCC efficiency of Ti_3Co cluster.

Sample	AQY	SCC
Ti_3Co-cluster	1.2%	0.038%

Table S7. Comparison of photocatalytic performance for H_2O_2 production.

Entry	Catalyst	Production rate ($\mu mol\ g^{-1}\ h^{-1}$)	Solvent	Irradiated Wavelength (nm)	AQY/ %	Reference
1	Ti_3Co cluster	1140	H_2O/IPA	⩾280	1.02%	This work
2	Ti_3Mn cluster	376	H_2O/IPA	⩾280	–	This work
3	AuPd/$BiVO_4$/MnOOH(0.5%)	143	PBS/H_2O	⩾420	1.07%	[14]
4	$BiVO_4$/MnOOH(0.5%)	47	PBS/H_2O	⩾420	–	[15]
5	TiO_2/MIL 125-NH_2/Ti_3C_2	278	H_2O/IPA	⩾420	–	[16]
6	SCN/TiO_2	425.6	H_2O	⩾420	–	[17]
7	Co-N-C/SAPDI	894	H_2O/Phenol	⩾420	–	[18]
8	Co@TiO_2	1700	H_2O/CH_3OH	=400	_	[19]
9	TiO_2	3.3	H_2O/benzyl alcohol	＞280	29.1%	[20]
10	CoPi/rGO/TiO_2	1500	H_2O/2-propanol	⩾320	–	[21]
11	MIL-125-NH_2	800	H_2O/benzyl alcohol	>420	_	[22]
12	CoSA/PCN	310	H_2O/IPA	>300	_	[23]

References

[1] L. Acharya, L. Biswal, B. P. Mishra, S. Das, S. Dash and K. Parida, *Chem. Eur. J*, 2024, **30**.

[2] P. P. Sarangi, K. K. Das, J. Sahu, U. A. Mohanty, D. P. Sahoo and K. Parida, *Inorg. Chem*, 2025, **64**, 2723-2736.

[3] G. Kresse., *Phys Rev*, 1996, **54**, 11169.

[4] G. Kresse., *Phys Rev B*, 1999, **59**, 1758e75.

[5] M. Ernzerhof., *J Chem Phys.*, 1999, **110**, 5029e36.

[6] K. Momma and F. Izumi, *J Appl Crystallogr*, 2011, **44**, 1272-1276.

[7] V. Wang, N. Xu, J.-C. Liu, G. Tang and W.-T. Geng, *Comput. Phys. Commun*, 2021, **267**, 108033.

[8] M. J. Frisch, G. W. Trucks, H. B. Schlegel, G. E. Scuseria, M. A. Robb, J. R. Cheeseman, G. Scalmani, V. Barone, G. A. Petersson, H. Nakatsuji, X. Li, M. Caricato, A. V. Marenich, J. Bloino, B. G. Janesko, R. Gomperts, B. Mennucci, H. P. Hratchian, J. V. Ortiz, A. F. Izmaylov, J. L. Sonnenberg, Williams, F. Ding, F. Lipparini, F. Egidi, J. Goings, B. Peng, A. Petrone, T. Henderson, D. Ranasinghe, V. G. Zakrzewski, J. Gao, N. Rega, G. Zheng, W. Liang, M. Hada, M. Ehara, K. Toyota, R. Fukuda, J. Hasegawa, M. Ishida, T. Nakajima, Y. Honda, O. Kitao, H. Nakai, T. Vreven, K. Throssell, J. A. Montgomery Jr., J. E. Peralta, F. Ogliaro, M. J. Bearpark, J. J. Heyd, E. N. Brothers, K. N. Kudin, V. N. Staroverov, T. A. Keith, R. Kobayashi, J. Normand, K. Raghavachari, A. P. Rendell, J. C. Burant, S. S. Iyengar, J. Tomasi, M. Cossi, J. M. Millam, M. Klene, C. Adamo, R. Cammi, J. W. Ochterski, R. L. Martin, K. Morokuma, O. Farkas, J. B. Foresman and D. J. Fox, *Journal*, 2016.

[9] P. J. Stephens, F. J. Devlin, C. F. Chabalowski, M. J. Frisch, *J. Phys. Chem*. 1994, **98**, 11623-11627.

[10] S. Grimme, J. Antony, S. Ehrlich, H. Krieg, *J. Chem. Phys*. 2010, **132**, 154104.

[11] A. D. Becke, *J. Chem. Phys*. 1993, **98**, 1372-1377.

[12] C. T. Lee, W. T. Yang, R. G. Parr, *Phys. Rev. B*, 1988, **37**, 785-789.

[13] A. D. Becke, *Phys. Rev. A* ,1988, **38**, 3098-3100.

[14] X. Yin, H. Shi, Y. Wang, X. Wang, P. Wang and H. Yu, *Acta Phys. Chim. Sin.*, 2024, **40**.

[15] Y. Yang, Z. Zeng, G. Zeng, D. Huang, R. Xiao, C. Zhang, C. Zhou, W. Xiong, W. Wang, M. Cheng, W. Xue, H. Guo, X. Tang and D. He, *Appl. Catal. B Environ*, 2019, **258**, 117956.

[16] Z. Jiang, Q. Long, B. Cheng, R. He and L. Wang, *J Mater Sci Technol*, 2023, **162**, 1-10.

[17] L. Ning, X. Chen, Z. Wang and J. Xu, *Appl. Catal. B Environ*, 2023, **324**, 122282.

[18] T. Baran, S. Wojtyła, A. Minguzzi, S. Rondinini and A. Vertova, *Appl. Catal. B Environ*, 2019, **244**, 303-312.

[19] Y. Shiraishi, S. Kanazawa, D. Tsukamoto, A. Shiro, Y. Sugano and T. Hirai, *ACS Catalysis*, 2013, **3**, 2222-2227.

[20] G.-h. Moon, W. Kim, A. D. Bokare, N.-e. Sung and W. Choi, *Energy Environ. Sci.*, 2014, **7**, 4023-4028.

[21] Y. Isaka, Y. Kawase, Y. Kuwahara, K. Mori and H. Yamashita, *Angewandte Chemie International Edition*, 2019, **58**, 5402-5406.
[22] Y. Shen, Y. Yao, C. Zhu, J. Wu, L. Chen, Q. Fang and S. Song, *Chemical Engineering Journal*, 2023, **475**, 146383.